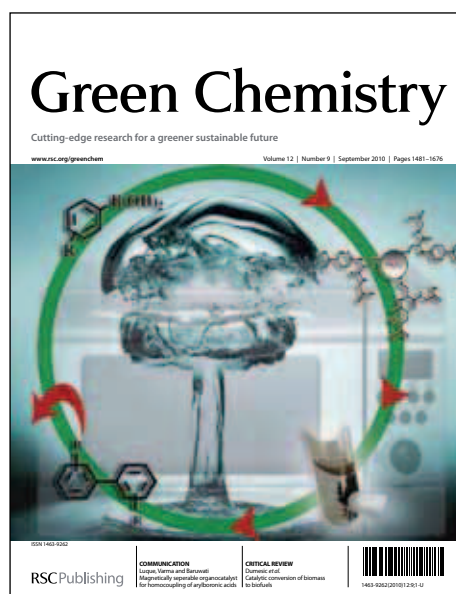


# Green Chemistry

## Accepted Manuscript

This article can be cited before page numbers have been issued, to do this please use: D. Yin, Y. Kong and L. Zhao, *Green Chem.*, 2013, DOI: 10.1039/C3GC40772A.



This is an *Accepted Manuscript*, which has been through the RSC Publishing peer review process and has been accepted for publication.

*Accepted Manuscripts* are published online shortly after acceptance, which is prior to technical editing, formatting and proof reading. This free service from RSC Publishing allows authors to make their results available to the community, in citable form, before publication of the edited article. This *Accepted Manuscript* will be replaced by the edited and formatted *Advance Article* as soon as this is available.

To cite this manuscript please use its permanent Digital Object Identifier (DOI®), which is identical for all formats of publication.

More information about *Accepted Manuscripts* can be found in the [Information for Authors](#).

Please note that technical editing may introduce minor changes to the text and/or graphics contained in the manuscript submitted by the author(s) which may alter content, and that the standard [Terms & Conditions](#) and the [ethical guidelines](#) that apply to the journal are still applicable. In no event shall the RSC be held responsible for any errors or omissions in these *Accepted Manuscript* manuscripts or any consequences arising from the use of any information contained in them.

## Graphical Abstract

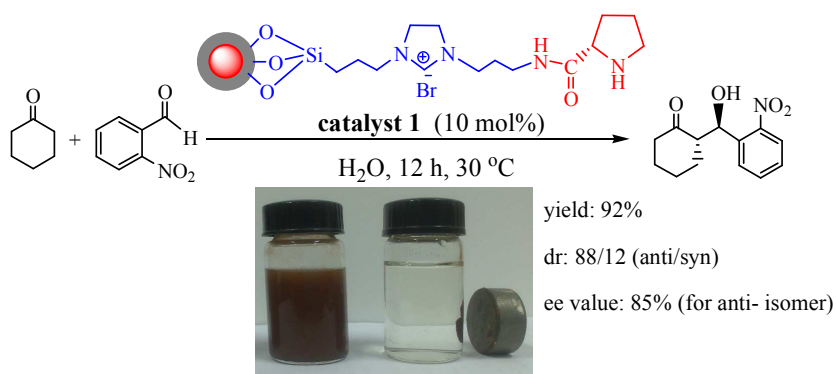
L-Proline supported on ionic liquid-modified magnetic nanoparticles  
as a highly efficient and reusable organocatalyst for direct  
asymmetric aldol reaction in water

Yu Kong<sup>a</sup>, Rong Tan,<sup>\*a</sup> Lili Zhao,<sup>a</sup> Chengyong Li<sup>a</sup> and Donghong Yin,<sup>\*a,b</sup>

<sup>a</sup> Institute of Fine Catalysis and Synthesis, Key Laboratory of Chemical Biology and Traditional Chinese Medicine Research (Ministry of Education), Hunan Normal University, Changsha, Hunan, 410081, China

<sup>b</sup> Technology Center, China Tobacco Hunan Industrial Corporation, NO. 426 Laodong Road, Changsha, Hunan, 410014, China

L-proline was covalently grafted on the MNPs through an imidazolium-based IL linker, which provided a highly efficient and magnetically recoverable L-proline catalyst for the asymmetric direct aldol reaction in water.



\* Corresponding authors. Fax: +86-731-8872531. Tel: +86-731-8872576

E-mail: yiyangtanrong@126.com (R. Tan); yindh@hunnu.edu.cn (D. Yin)

Cite this: DOI: 10.1039/c0xx00000x

www.rsc.org/xxxxxx

ARTICLE TYPE

# L-Proline supported on ionic liquid-modified magnetic nanoparticles as a highly efficient and reusable organocatalyst for direct asymmetric aldol reaction in water

Yu Kong<sup>a</sup>, Rong Tan,<sup>\*a</sup> Lili Zhao<sup>a</sup> and Donghong Yin<sup>\*a,b</sup><sup>5</sup> Received (in XXX, XXX) Xth XXXXXXXXX 200X, Accepted Xth XXXXXXXXX 200X

DOI: 10.1039/b000000x

Grafting L-proline on imidazolium-based ionic liquid (IL)-functionalized magnetic nanoparticles afforded a magnetically recoverable L-proline catalyst. Characterization technologies suggested the presence of an L-proline backbone, an IL linker, and a magnetic ferrite core in the catalyst. The resulting L-proline catalyst was efficient for direct asymmetric aldol reaction in water without need for organic solvents and co-catalysts. Such efficiency is attributed to the fact that the IL moiety facilitated the accessibility of hydrophobic reactants to active sites in water and stabilized the formed enamine intermediate during the reaction. High activity (yield = 92%), diastereoselectivity (dr; 88/12) and enantioselectivity (ee; 85%) were obtained using 10 mol% catalyst for the reaction between cyclohexanone and 2-nitrobenzaldehyde within 12 h, where the pristine L-proline and IL-free counterpart were almost inactive. The catalyst was easily separated using a permanent magnet externally and can be reused for several times without significant loss of activity.

## 15 Introduction

Direct asymmetric aldol reactions between unmodified ketones and aldehydes are useful carbon-carbon bond-forming reactions that serve as a convenient method of synthesizing chiral organic compounds.<sup>1</sup> Proline is gaining increased attention in direct asymmetric aldol reactions because it is efficient, environmentally benign, easily accessible, and available in both enantiomeric forms.<sup>2</sup> Unlike natural aldolases that are efficient for the aldol reaction in water, proline is an organocatalyst typically used with an excess of reacting ketone,<sup>3</sup> organic solvent,<sup>2a, 2g, 4</sup> or ionic liquids (ILs).<sup>5</sup> If bulk water is used as the reaction medium, low reactivity or even no reaction progress is detected probably because of the limited affinity between the hydrophobic reactants and proline catalyst in water.<sup>2e, 6</sup> Long-chain hydrocarbon fragments have been introduced into the framework of proline to make hydrophobic substrates compatible in aqueous medium. The resulting yield is high and the selectivity is excellent, but efficient recovery of catalyst and high purity of

product are difficult to achieve.<sup>2e</sup> ILs are also used as alternative modifiers to make L-proline efficient and reusable in aqueous direct asymmetric aldol reactions.<sup>6c, 7</sup> However, the separation process of IL-tagged L-proline is undesirable. Excessive organic solvent is often required to selectively precipitate the catalyst out of the reaction mixture. Thus far, the preparation of an efficient and recoverable L-proline catalyst for direct asymmetric aldol reaction in water remains challenging.

Magnetic nanoparticles (MNPs) especially Fe<sub>3</sub>O<sub>4</sub> coated with silica (SiO<sub>2</sub>@Fe<sub>3</sub>O<sub>4</sub>) are emerging as interesting supports for the immobilization of homogeneous catalysts.<sup>8</sup> Different from many traditional porous supports, the nonporous MNPs induce the distribution of catalytically active sites throughout the outer surface; thus, the pore diffusion constraint is practically avoided. Importantly, magnetic separation renders the recovery of catalysts from liquid-phase reactions much easier and more efficient than by filtration and centrifugation. Some pioneer contributions of organocatalysis are also known in this emerging field.<sup>9, 4b</sup> For example, Luo *et al.*<sup>9b</sup> prepared MNP-supported chiral primary amine catalysts that are efficient and recyclable for direct asymmetric aldol reaction. This successful preparation paves the way for a range of MNP-supported asymmetric organocatalysts. Lately, Yang *et al.*<sup>4b</sup> covalently grafted L-proline onto SiO<sub>2</sub>@Fe<sub>3</sub>O<sub>4</sub> nanoparticles and proved that the MNP-based L-proline catalyst is efficient for asymmetric aldol reaction in ethanol and can be recovered simply by magnetic separation. However, the catalyst is also almost inactive when only water is used as the reaction medium because of the limited mass transfer. This problem can be solved by attaching L-proline to an IL-modified MNP. Apart from the active role of an IL linker in the overall reaction mechanism, such linker may fine tune the dispersion of the supported catalyst in water and make the catalyst more compatible with organic substrates and solvent.

<sup>\* a</sup> Institute of Fine Catalysis and Synthesis, Key Laboratory of Chemical Biology and Traditional Chinese Medicine Research (Ministry of Education), Hunan Normal University, Changsha, Hunan, 410081, China;

<sup>b</sup> Technology Center, China Tobacco Hunan Industrial Corporation, NO. 426 Laodong Road, Changsha, Hunan, 410014, China.

Fax: +86-731-8872531; Tel: +86-731-8872576; E-mail: yiyangtanrong@126.com (R. Tan) or yindh@hunnu.edu.cn (D. Yin)

†Electronic Supplementary Information (ESI) available: General procedure for the direct asymmetric aldol reaction, detailed NMR spectra and HPLC analysis for the aldol products. See DOI: 10.1039/b000000x/

Therefore, the problems associated with the transport of reactants to catalytic sites can be circumvented.

In this study, we reported a novel L-proline catalyst composed of a  $\text{Fe}_3\text{O}_4$  core, which made the catalyst magnetically recoverable, and a shell consisting of L-proline appended by an amine-functionalized IL. The novel L-proline catalyst (**L-proline-IL-SiO<sub>2</sub>@Fe<sub>3</sub>O<sub>4</sub>**) was efficient in direct asymmetric aldol reaction in water without need of organic solvents and co-catalysts. Furthermore, the catalyst can be easily separated with an external magnet without using extra organic solvents or additional filtration steps. Thus, the technology is green and solves the problems associated with mass transfer and catalyst recycling in aqueous aldol reaction.

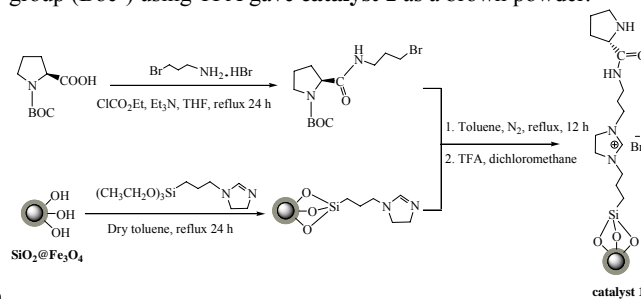
## Results and Discussion

### Preparation and Characterization of Catalysts

MNPs are used as heterogeneous catalytic supports because of their high surface area that result in high catalyst loading capacity, high dispersion, outstanding stability, and convenient catalyst recycling.<sup>8b-d</sup> MNPs generally require further modification to confer high dispersion in a range of media for catalytic reactions and/or sufficient stability under the harsh conditions needed for catalytic reactions and catalyst recycling.<sup>8c</sup> ILs, as modifiers in support systems, fine tune the surface properties of the support and transfer the properties of the ILs to materials,<sup>10</sup> which are expected to improve the compatibility of the hydrophobic substrates in an aqueous system. Imidazolium-based ILs have also been found to activate L-proline in direct asymmetric reactions.<sup>2f</sup> Thus, we decided to immobilize L-proline on imidazolium-based IL-functionalized MNPs by covalent linkage to produce efficient and magnetically recoverable L-proline catalysts for direct asymmetric aldol reaction in water. Given that the five-membered nitrogen containing the L-proline heterocycle is regarded as one of the "privileged" backbones of the asymmetric reaction,<sup>2a, 11</sup> we designed a strategy in the present study to covalently tether the L-proline derivative containing the intact "privileged" chiral pyrrolidine unit and a halogenated hydrocarbon group to imidazole-modified MNPs by forming an imidazolium-based IL linker.

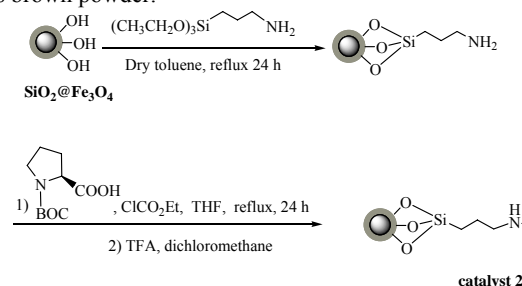
The preparation of **L-proline-IL-SiO<sub>2</sub>@Fe<sub>3</sub>O<sub>4</sub>** (denoted as **catalyst 1**) is shown in Scheme 1.  $\text{SiO}_2@\text{Fe}_3\text{O}_4$  was readily synthesized by a chemical co-precipitating method similar to a previously reported one,<sup>12</sup> followed by an  $\text{SiO}_2$ -coating procedure.<sup>13</sup> N-tert-butoxycarbonyl-L-proline (N-Boc-L-proline) was synthesized according to a procedure described in reference.<sup>14</sup> First, 3-bromopropylamine liberated from 3-bromopropylamine hydrobromide by NaOH aqueous reaction was directly reacted with N-Boc-L-proline in the presence of triethylamine and ethyl chloroformate, thereby affording the corresponding N-Boc-L-prolinamide-derived brominated hydrocarbon. Then, the bifunctional alkoxy silane reagent of N-[3-(triethoxysilyl)propyl]-4,5-dihydroimidazole was used to modify MNPs through the formation of Si–O bonds based on the reaction of alkoxy with the abundant surface hydroxyl groups (–OH) on  $\text{SiO}_2@\text{Fe}_3\text{O}_4$ . The successive alkylation of the N-alkylimidazole group on the modified MNPs with the brominated hydrocarbon group (–C<sub>3</sub>H<sub>6</sub>Br) in the L-proline derivative induced

the N-Boc-L-proline moiety to covalently tether onto the surface of the silica magnetic microspheres. Removal of the protecting group (Boc-) using TFA gave **catalyst 1** as a brown powder.



Scheme 1 Synthesis of the catalyst 1.

For comparison, the IL-free counterpart of **L-proline-NH<sub>2</sub>-SiO<sub>2</sub>@Fe<sub>3</sub>O<sub>4</sub>** (denoted as **catalyst 2**), in which L-proline was directly grafted onto amino-functionalized magnetic microspheres, was also prepared according to a preparation procedure similar to that of **catalyst 1**, as shown in Scheme 2. During the procedure, the organosiloxane of 3-aminopropyltriethoxysilane was used instead of N-[3-(triethoxysilyl)propyl]-4,5-dihydroimidazole to modify the surface of  $\text{SiO}_2@\text{Fe}_3\text{O}_4$ . The abundant surface amino groups (–NH<sub>2</sub>) present on  $\text{SiO}_2@\text{Fe}_3\text{O}_4$  were readily reacted with the carboxyl group of N-Boc-L-proline by the mixed anhydride method,<sup>14</sup> giving the Boc-protected L-prolinamide- $\text{SiO}_2@\text{Fe}_3\text{O}_4$ . Removal of the protecting group (Boc-) also afforded **catalyst 2** as brown powder.



Scheme 2 Synthesis of the catalyst 2.

The magnetic **catalyst 1** can be well dispersed in both aqueous and organic solvents to form a stable suspension in the absence of a magnetic field (Fig. 1b). We speculated that the high dispersion was related to the nanoscale size of support and the special solubility of the imidazolium-based IL coating. Actually, **catalyst 1** exhibited better dispersion in water than the IL-free counterpart, as shown in Fig. 1 (Figs. 1b vs. 1a).

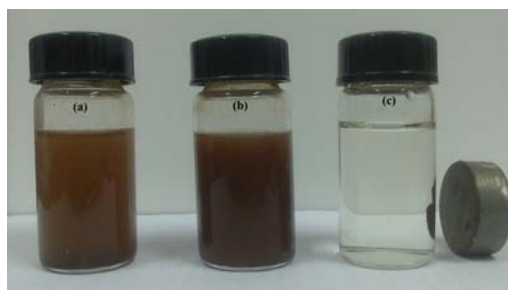


Fig. 1 Photographs of the dispersion of **catalyst 2** (a) and **catalyst 1** (b) in water and the separation of **catalyst 1** with an external magnet (c).

The high dispersion of the catalyst in water and easy accessibility to the active sites result in high reactivity in aqueous direct asymmetric aldol reaction. Interestingly, the nanoparticles of **catalyst 1** can be aggregated using moderate magnetic field strengths (Fig. 1c). This observation suggested that the magnetic catalyst was easy to separate from the reaction mixtures using a permanent magnet externally through a magnetic concentration step.

### Characterization of Samples

#### TEM

TEM images were used to obtain information on the particle size and morphology of as-prepared samples of  $\text{SiO}_2@\text{Fe}_3\text{O}_4$ , **catalyst 1**, and **catalyst 2**. The typical TEM images are shown in Fig. 2. Particles with an approximately spherical shape and average diameter of ca. 14 nm were observed on the image of  $\text{SiO}_2@\text{Fe}_3\text{O}_4$  (Fig. 2a). The diameter of the particles is somewhat larger than the typical diameter of bare  $\text{Fe}_3\text{O}_4$  prepared by chemical co-precipitation (ca. 10 nm),<sup>15</sup> suggesting that these core-shell samples of  $\text{SiO}_2@\text{Fe}_3\text{O}_4$  were coated by a thin silica layer ca. 4 nm thick. This type of silica coating reduced the irreversible aggregation of individual particles and provided abundant reaction sites for grafting L-proline. The size and morphology of the MNPs did not significantly change after anchoring the L-proline moiety onto the silica shell using an imidazolium-based IL linker (Fig. 2b). This finding suggested that the magnetic ferrite core was intact during immobilization and that the functional reaction occurred only on the particle surface. Meanwhile, no detectable outer IL-tagged L-proline shell within the sensitivity limit of TEM (Fig. 2b) was observed. A reasonable explanation may be the existence of a monolayer of IL-tagged L-proline shell, which was too thin to be recognized. The structural features of **catalyst 1** particularly the good dispersion of catalytically active centers on the surface made the catalyst efficient in aqueous aldol reaction. The prepared IL-free counterpart (**catalyst 2**) also showed an approximately spherical particle morphology with an average particle diameter of ca. 14 nm in the TEM image (Fig. 2c).

### Particle Size Distribution Analysis

In order to determine the change in the size of the nanoparticles after modification, the particle size distribution of  $\text{SiO}_2@\text{Fe}_3\text{O}_4$ , **catalyst 1**, and **catalyst 2** was measured by a MS2000 Laser Particle Size Analyzer, as shown in Fig. 3. The samples for measurement were sonicated in deionized water for 1.5 h. It was found that the mean hydrodynamic diameter of  $\text{SiO}_2@\text{Fe}_3\text{O}_4$  (ca. 19.8 nm) was greater than the particles size estimated by TEM images (ca. 14 nm) due to the presence of hydration layer on the particles (Fig. 3a).<sup>16</sup> The modification of organic moiety on the surface indeed resulted in an increase in the average hydrodynamic diameter. **Catalyst 1** with an IL-tagged L-proline shell showed the mean hydrodynamic diameter of 27.5 nm (Fig. 3b), while the IL-free counterpart of **catalyst 2** showed a smaller average hydrodynamic diameter (ca. 23.8 nm) than that of the **catalyst 1** (Fig. 3c vs. 3b).

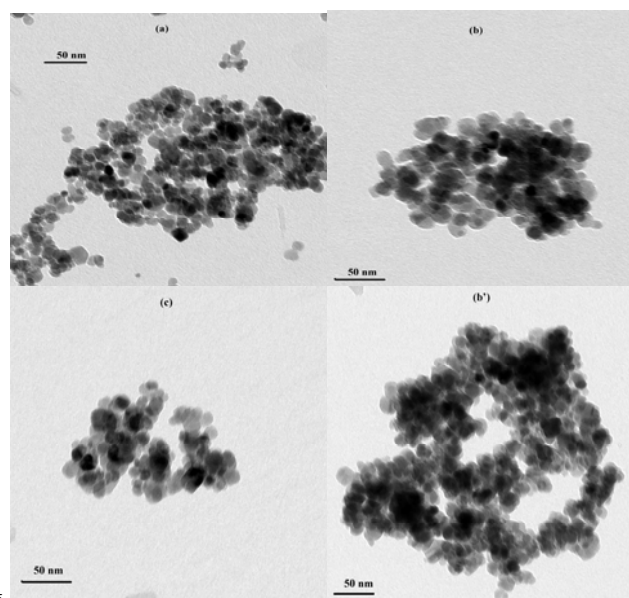


**Fig. 2** TEM images of the  $\text{SiO}_2@\text{Fe}_3\text{O}_4$  (a), **catalyst 1** (b), **catalyst 2** (c) and the **catalyst 1** after the 5th reaction (b').

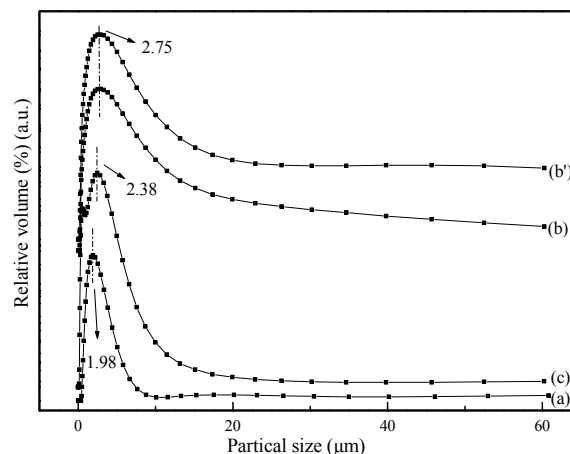


**Fig. 3** Hydrodynamic diameter of the  $\text{SiO}_2@\text{Fe}_3\text{O}_4$  (a), **catalyst 1** (b), **catalyst 2** (c) and the **catalyst 1** after the 5th reaction (b').

### XRD

Fig. 4 displays the high-angle powder XRD patterns of **catalysts 1** and **2** together with those of  $\text{SiO}_2@\text{Fe}_3\text{O}_4$  and L-proline. Fig. 4c shows that the XRD pattern of  $\text{SiO}_2@\text{Fe}_3\text{O}_4$  had the typical peaks at  $30.08^\circ$ ,  $35.42^\circ$ ,  $43.08^\circ$ ,  $53.56^\circ$ ,  $56.98^\circ$ , and  $62.62^\circ$ , which corresponded to the (220), (311), (400), (422), (511), and (440) reflections of pure  $\text{Fe}_3\text{O}_4$  with a spinel structure, respectively.<sup>8f</sup> These characteristic peaks were also present in the powder XRD patterns of the MNP-based **catalysts 1** and **2**, suggesting that the surface modification of MNPs did not significantly affect the phase composition of  $\text{SiO}_2@\text{Fe}_3\text{O}_4$  (Figs. 4a and 4b vs. Fig. 4c). Moreover, compared with the XRD pattern of pristine L-proline, the XRD patterns of **catalysts 1** and **2** did not show any distinct diffraction peak corresponding to the crystalline L-proline phase (Figs. 4a and 4b vs. Fig. 4d), which confirmed the high dispersion of L-proline on the surface of MNPs.

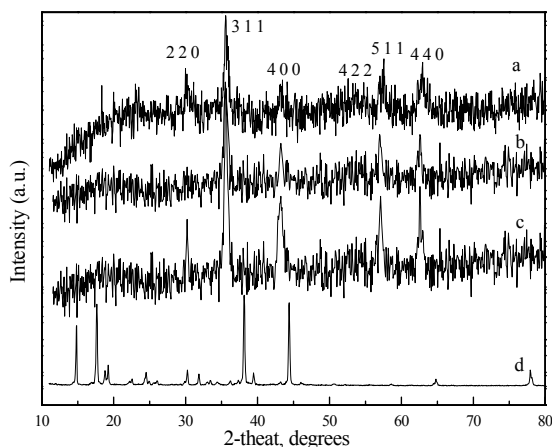


**Fig. 4** Powder X-ray diffraction patterns of **catalyst 1** (a), **catalyst 2** (b),  $\text{SiO}_2@Fe_3O_4$  (c), and L-proline (d).

### FT-IR

The covalent binding of L-proline to the surface of IL-modified  $\text{SiO}_2@Fe_3O_4$  in **catalyst 1** was further confirmed by FT-IR analysis. Fig. 5 shows the FT-IR spectra of **catalysts 1** and **2**, as well as imidazole-modified  $\text{SiO}_2@Fe_3O_4$  for comparison. The FT-IR spectrum of imidazole-modified  $\text{SiO}_2@Fe_3O_4$  had the characteristic Fe–O vibrations at around  $581\text{ cm}^{-1}$  and the characteristic Si–O vibrations at around  $1131\text{ cm}^{-1}$ .<sup>17</sup> The presence of the imidazole group on the surface of  $\text{SiO}_2@Fe_3O_4$  was evident from the characteristic bands at  $1655$  (–NH– stretching vibration of imidazole ring),  $2864$ , and  $2941\text{ cm}^{-1}$  (C–H and/or N–H stretching vibration) (Fig. 5a).<sup>18</sup> The imidazole modifier was responsible for the covalent anchoring of L-proline on  $\text{SiO}_2@Fe_3O_4$  by forming an imidazolium-based IL linker, as shown in Scheme 1. After L-proline anchoring, a new band at around  $1680\text{ cm}^{-1}$  appeared in the FT-IR spectrum of **catalyst 1**, which was the characteristic stretching vibration of the C=O band in the –CONH– group (Fig. 5b).<sup>19</sup> The –CONH– group in **catalyst 1** suggested the successful introduction of the L-prolinamide derivative moiety to imidazole-modified  $\text{SiO}_2@Fe_3O_4$ . However, the characteristic stretching vibrations of the five-membered nitrogen containing the L-proline heterocycle overlapped with the stretching modes of the imidazolium group. The FT-IR spectrum of **catalyst 2** was similar to that of **catalyst 1** (Fig. 5c vs. 5b), except for the absence of the characteristic –NH– stretching vibration of imidazole ring (near  $1655\text{ cm}^{-1}$ ). The difference was related to the absence of the imidazolium-based IL moiety in the framework of **catalyst 2**. The characteristic band derived from the stretching vibration mode of C=O in –CONH– (at around  $1680\text{ cm}^{-1}$ ) in the FT-IR spectrum of **catalyst 2** provided direct evidence that L-proline was directly anchored onto amino-functionalized MNPs by forming L-prolinamide (Fig. 5c), as shown in Scheme 2. Notably, compared with **catalyst 2**, a significant feature observed for **catalyst 1** was the presence of the imidazolium-based IL linker that positively affected the catalytic performance of L-proline catalyst in the aldol reaction in water.

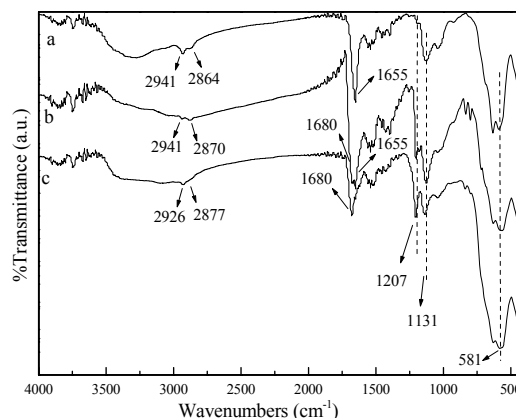


**Fig. 5** FT-IR spectra of N-[3-(triethoxysilyl)propyl]-4,5-dihydroimidazole modified MNPs (a), **catalyst 1** (b) and **catalyst 2** (c).

### Thermal Analysis

Thermal analysis was performed to monitor the decomposition profiles of **catalyst 1**, **catalyst 2**, and pristine L-proline for comparison. The results are shown in Fig. 6. **Catalyst 1** showed six distinct steps of weight losses in the combined TG-DTG curves upon heating from room temperature to  $800\text{ }^\circ\text{C}$  under airflow (Fig. 6b). The first weight loss at  $90\text{ }^\circ\text{C}$  was due to the removal of surface-adsorbed water. The second weight loss at  $141\text{ }^\circ\text{C}$ , which was absent in the combined TG-DTG curves of **catalyst 2** (Fig. 6b vs. 6a), accounted for the release of bromine anions in the IL moiety as hydrogen bromine.<sup>20</sup> The third weight loss at  $170\text{--}244\text{ }^\circ\text{C}$  was probably due to the loss of structural water within amorphous  $\text{SiO}_2$ .<sup>4b</sup> The fourth weight loss at  $245\text{--}360\text{ }^\circ\text{C}$  was assigned to the successive cleavage of L-proline moiety. Interestingly, the decomposition temperature of the supported L-proline moiety increased compared with that of pristine L-proline (Fig. 6b vs. 6c), because of the mutual stabilization of L-proline and MNP support. This finding indirectly proved the covalent linkage of L-proline moieties onto the surface of MNPs through the IL moiety. The L-proline content of **catalyst 1** was ca.  $0.45\text{ mmol/g}$ , which was estimated according to the weight loss within the temperature range. The fifth weight loss was at  $393\text{ }^\circ\text{C}$ , followed by an additional weight loss at  $480\text{ }^\circ\text{C}$  that extended up to ca.  $540\text{ }^\circ\text{C}$ . The two steps that were well distinguished in the DTG curve can be associated with the complete decomposition of the imidazolium-functionalized trialkoxysilane moiety.<sup>21</sup> The total weight loss was determined to be 29% for **catalyst 1**, and the non-removable residue was produced by the formation of iron oxide and silica in air at a high temperature. The IL-free counterpart of **catalyst 2** showed a decomposition profile similar to **catalyst 1**, except for the disappearance of the decomposition steps associated with the imidazolium-based IL moiety (Fig. 6a). TGA analysis revealed that the L-proline content of **catalyst 2** was ca.  $0.41\text{ mmol/g}$ . The total weight loss of **catalyst 2** was determined to be 11%. Separated TG-DTG curves of **catalyst 1**, **catalyst 2**, and pristine L-proline are provided in the Supplementary material (Fig. S42).

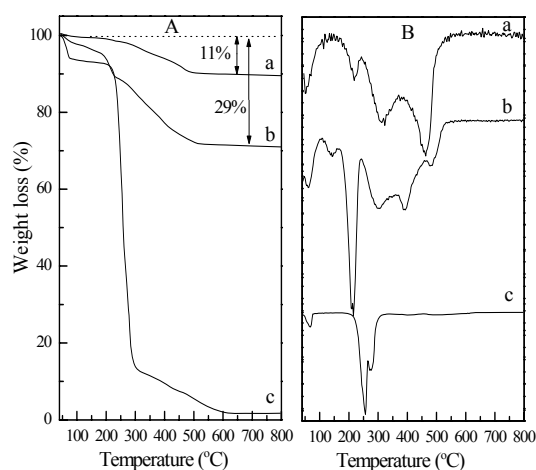


Fig. 6 Thermogravimetric (A) and differential thermogravimetric (B) results of **catalyst 2** (a), **catalyst 1** (b), and pristine L-proline (c).

### Catalytic Performances

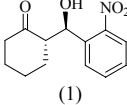
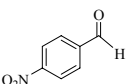
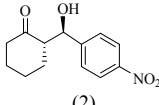
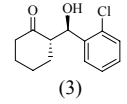
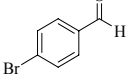
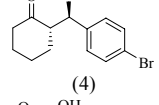
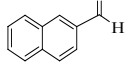
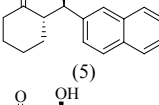
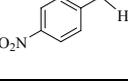
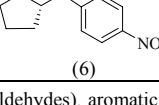
Catalytic asymmetric aldol reactions in water have been extensively researched in recent years because water is an inexpensive, safe, and environmentally benign reaction medium that often exerts a synergistic effect on reactivity and selectivity.<sup>11a,22</sup> Although the addition of a small amount of water may accelerate reactions and/or improve enantioselectivity,<sup>23</sup> water as a reaction solvent often results in a low yield with low or no enantioselectivity because of poor mass transfer.<sup>2e,6</sup> The IL-tagged **catalyst 1** was designed for direct asymmetric aldol reaction performed in water. We proposed that the presence of imidazolium-based IL favored the reagents' diffusion toward active sites and enhanced the catalytic activity of **catalyst 1** in aqueous aldol addition. Hydrophobic cycloalkanones were selected as the aldol donor to investigate the catalytic performance of **catalyst 1** in direct asymmetric aldol reaction in water. The results are summarized in Table 1. The absolute configurations of the products were deduced by comparing the HPLC retention times with reported values.<sup>24</sup>

Interestingly, **catalyst 1** was efficient for the direct asymmetric aldol reaction of cyclohexanone with 2-nitrobenzaldehyde in water. About 10 mol% of the novel **catalyst 1** was sufficient for affording an almost quantitative yield (92%) of the aldol product with good diastereoselectivity (up to 88/12, anti/syn) and enantioselectivity (up to 85% for the *anti*-isomer) in the direct asymmetric aldol reaction of cyclohexanone with 2-nitrobenzaldehyde within 12 h (Table 1, entry 3). However, no reaction progress was detected even after 48 h in water when the reaction was catalyzed by pristine L-proline (Table 1, entry 2). The results suggested that the imidazolium-based IL modified MNPs created a microenvironment advantageous for reactant diffusion in water. The parent SiO<sub>2</sub>@Fe<sub>3</sub>O<sub>4</sub> was found to be inactive for aqueous aldol reaction (Table 1, entry 1).

To elucidate the function of the imidazolium-based IL moiety in an aqueous reaction, an IL-free counterpart (**catalyst 2**) was prepared as a control catalyst by directly anchoring the L-proline moiety onto amino-modified MNPs. We noticed that **catalyst 2** offered a slightly higher yield of the desired aldol product than pristine L-proline probably because of the improved mass transfer originating from the hydrophobic alkyl spacer. However, **catalyst 2** was far less active than the IL-tagged **catalyst 1** under identical

reaction conditions (Table 1, entry 4 vs. 3). Only 10% yield of the aldol product was obtained over **catalyst 2** within 12 h (Table 1, entry 4). This observation clearly indicated that the imidazolium-based IL moiety played a critical role in aqueous direct asymmetric aldol reaction. The midway addition of 1-methyl-3-butylimidazolium bromine IL (equivalent to the IL amount in **catalyst 1**) to the **catalyst 2**-mediated aldol reaction system indeed led to increased yield from 10% to 17% (Table 1, entry 5 vs. 4), whereas the yield was far lower than that obtained over **catalyst 1** (Table 1, entry 5 vs. 3). Thus, the proximity of the IL unit to the active site made the active center a kind of IL that rendered catalytic sites more accessible, thereby tuning **catalyst 1** into an efficient catalyst for this reaction. In fact, apart from the compatibility, the high polarity and ionic character of the IL moiety exerted synergistic effects on stabilizing the formed enamine intermediate in the direct asymmetric aldol reaction, which in turn improved the catalytic efficiency of L-proline.<sup>5c</sup>

Table 1 Direct asymmetric aldol reaction between cycloalkanones and aromatic aldehydes catalyzed by L-proline in water<sup>a</sup>

Entry	Catalyst	Substrate	Product	Yield <sup>b</sup> (%)	Anti/syn <sup>c</sup> (%)	ee <sup>d</sup> (%)
1	SiO <sub>2</sub> @Fe <sub>3</sub> O <sub>4</sub>			Trace	nd <sup>e</sup>	nd <sup>e</sup>
2	L-proline <sup>f</sup>			Trace	nd <sup>e</sup>	nd <sup>e</sup>
3	<b>Catalyst 1</b>			92	88:12	85
4	<b>Catalyst 2</b>			10	nd	nd
5	<b>Catalyst 2</b> <sup>g</sup>			17	nd	nd
6	<b>Catalyst 1</b>			96	76:24	75
7	<b>Catalyst 1</b>			75	99:1	89
8	<b>Catalyst 1</b>			55	89:11	82
9	<b>Catalyst 1</b>			30	98:2	45
10	<b>Catalyst 1</b>			90	33:67	86

<sup>a</sup> **Catalyst** (10 mol% of aromatic aldehydes), aromatic aldehyde (0.25 mmol), cycloalkanone (2.5 mmol), H<sub>2</sub>O (2 ml), 12 h, 30 °C. <sup>b</sup> Isolated yield after column chromatography. <sup>c</sup> Determined by <sup>1</sup>H NMR analysis. <sup>d</sup> Determined by HPLC (Daicel chiralpak AD column) on the *anti*-isomer product. <sup>e</sup> Not determined. <sup>f</sup> Pristine L-proline (10 mol% of 2-nitrobenzaldehyde), 2-nitrobenzaldehyde (0.25 mmol), cyclohexanone (2.5 mmol), H<sub>2</sub>O (2 ml), 48 h,

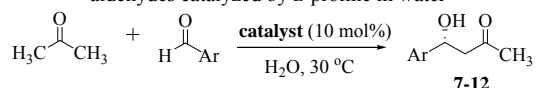
30 °C. <sup>8</sup> **Catalyst 2** (10 mol% of 2-nitrobenzaldehyde), 1-methyl-3-buthylimidazolium bromine (0.01 g, equivalent to the amount of IL in **catalyst 1**), 2-nitrobenzaldehyde (0.25 mmol), cyclohexanone (2.5 mmol), H<sub>2</sub>O (2 ml), 12 h, 30 °C.

Excellent performance of **catalyst 1** was also observed in the direct asymmetric aldol reaction of cyclohexanone with other aromatic aldehydes using water as a solvent. Table 1 shows that the aromatic aldehydes in all cases underwent reaction with cyclohexanone to produce the corresponding β-hydroxy ketone in moderate to high yields, diastereoselectivities, and ee values in water within 12 h. In particular, the aromatic aldehydes carrying strong electron-withdrawing groups such as nitro groups were good acceptors in the presence of **catalyst 1** (10 mol%) at room temperature. 2-Nitrobenzaldehyde gave the desired the corresponding aldols in excellent yield (92%) with good diastereoselectivity (88/12, anti/syn) and enantioselectivity (85% ee for the anti-isomer) (Table 1, entry 2). Unfortunately, attempts to change the substituting group positions onto the aromatic aldehydes resulted in lower diastereoselectivity (76/24, anti/syn) and ee (75% ee for the anti-isomer), although the yields remained good (96%) (Table 1, entry 6). These phenomena were probably due to the electronic and steric effects of aromatic aldehydes. The formation of aldol products was related to the electron-withdrawing capacity of the substituent group on aldehydes for the active aldehyde group and the steric hindrance at the 2-position on the aromatic ring for enantioface discrimination in the transition state.<sup>25</sup> The halogenated aromatic aldehydes gave moderate yields of the corresponding aldol products (55%–75%), although the excellent diastereoselectivities (89/11–99/1, anti/syn) and enantioselectivities (82–89% ee for the anti-isomer) were encouraging. Relatively bulkier aromatic aldehydes, such as 2-naphthaldehyde, were also less reactive for aldol condensation with cyclohexanone because of the steric hindrance originating from the 2-naphthyl group that did not favor nucleophilic attack. The reaction gave lower yield (30%) and ee (45% ee for the anti-isomer) but a high anti/syn diastereomeric ratio (98/2) (Table 1, entry 9). The hydrophobic cyclopentanone was also efficiently reacted with 2-nitrobenzaldehyde over **catalyst 1** (10 mol%) in water. A high yield of 90% was found within 12 h, whereas the dr and ee values of aldol were somewhat lower (Table 1, entry 10).

The remarkably enhanced catalytic efficiency of the novel **catalyst 1** due to the presence of the imidazolium-based IL moiety was also observed when the water-soluble acetone was used as the aldol donor in the aqueous reaction. The comparative results are summarized in Table 2. **Catalyst 1** had a higher efficiency than its IL-free counterpart **catalyst 2** in the aqueous direct asymmetric aldol reaction of acetone with various aromatic aldehydes bearing either electron-rich or electron-deficient substituents under identical conditions (Table 2, entry 1 vs. 2, entry 4 vs. 5, entry 7 vs. 8, entry 10 vs. 11, entry 13 vs. 14, and entry 16 vs. 17). The satisfactory results obtained from the reaction showed that the imidazolium-based IL moiety enhanced catalyst activity by increasing the yields and enantioselectivities of the corresponding aldol products. Notably, less yields and enantioselectivities over **catalyst 2** were also obtained in the reactions even though the reaction time was prolonged to 48 h (Table 2, entry 1 vs. 3, entry 4 vs. 6, entry 7 vs. 9, entry 10 vs. 12,

entry 13 vs. 15, and entry 16 vs. 18). Furthermore, electron-deficient aldehydes were found to be more favorable for the aldol reaction, affording the relevant aldols in excellent yields. An almost quantitative conversion of 2-nitrobenzaldehyde (93% yield of product **7**) was achieved over 10 mol% of **catalyst 1** in the aqueous reaction within 12 h (Table 2, entry 1). 4-Nitrobenzaldehyde exhibited reactivity similar to that of 2-nitrobenzaldehyde in aqueous aldol reaction (Table 2, entry 4). 2-Chlorobenzaldehyde and 4-bromobenzaldehyde smoothly underwent aldol reaction in water over **catalyst 1** (10 mol%), giving products **9** and **10** in 75% and 55% yields, respectively, with 77% ee values (Table 2, entries 7 and 10). Electron-rich aldehydes, such as 4-acetamidobenzaldehyde, were less active under the studied conditions (Table 2, entry 13). The relatively bulkier 2-naphthaldehyde also showed a low yield (35%) even though the enantioselectivity (82% ee) can be tolerated (Table 2, entry 16).

**Table 2** Direct asymmetric aldol reaction between acetone and aromatic aldehydes catalyzed by L-proline in water<sup>a</sup>



Entry	Catalyst	Substrate	Product	Yield <sup>b</sup> (%)	ee (%)
1	<b>Catalyst 1</b>			93	79
2	<b>Catalyst 2</b>			60	51
3	<b>Catalyst 2</b> <sup>c</sup>			88	51
4	<b>Catalyst 1</b>			96	70
5	<b>Catalyst 2</b>			65	50
6	<b>Catalyst 2</b> <sup>c</sup>			90	51
7	<b>Catalyst 1</b>			75	77
8	<b>Catalyst 2</b>			45	49
9	<b>Catalyst 2</b> <sup>c</sup>			50	47
10	<b>Catalyst 1</b>			55	77
11	<b>Catalyst 2</b>			35	45
12	<b>Catalyst 2</b> <sup>c</sup>			45	44
13	<b>Catalyst 1</b>			35	83
14	<b>Catalyst 2</b>			20	46
15	<b>Catalyst 2</b> <sup>c</sup>			27	46
16	<b>Catalyst 1</b>			35	82
17	<b>Catalyst 2</b>			15	44
18	<b>Catalyst 2</b> <sup>c</sup>			25	43

<sup>a</sup> **Catalyst 1** (10 mol% of aromatic aldehydes), aromatic aldehyde (0.25 mmol), acetone (2.5 mmol), H<sub>2</sub>O (2 ml), 12 h, 30 °C. <sup>b</sup> Isolated yield after column chromatography. <sup>c</sup> **Catalyst 2** (10 mol% of aromatic aldehydes), aromatic

aldehyde (0.25 mmol), acetone (2.5 mmol), H<sub>2</sub>O (2 ml), 48 h, 30 °C. <sup>d</sup> Ee was determined by HPLC (Daicel chiralpak OB-H column) on pure products. <sup>e</sup> Ee value was determined by HPLC (Daicel chiralpak AD column) on pure products.

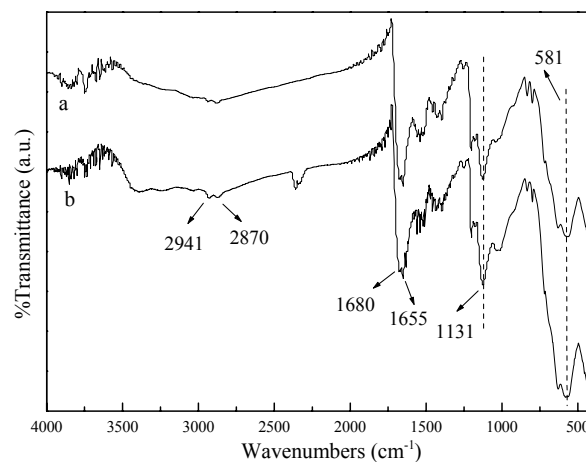
5 Apart from the excellent catalytic efficiency in aqueous aldol reaction, another important feature of the designed **catalyst 1** was its easy and reliable separation using an appropriate magnetic field. Upon completion of the reaction, the heterogeneous  
10 **catalyst 1** can be quantitatively recovered from the reaction mixture using an external magnetic field, as shown in Fig. 1 (Fig. 1c). The aqueous phase was then separated from the magnetic catalyst by decantation. Notably, although ethyl acetate was used to extract a small amount of aldols from the reaction solution in  
15 the present work, this approach was expected in large-scale industrial processes, in which the oily product phase can be directly separated from water without using any organic solvent. **Catalyst 1** that was stationary inside the vessel can be readily recycled by adding fresh reaction substrates.

20 Table 3 shows the results of the recovery and reusability of **catalyst 1** in the direct asymmetric aldol reaction of cyclohexanone with 2-nitrobenzaldehyde in water. The novel **catalyst 1** can be recycled for up to five times with no appreciable decrease in yield and selectivity of the aldol product,  
25 which demonstrated that the prepared **catalyst 1** possessed excellent stability and reusability. The reaction was completely stopped by catalyst removal. Elementary analysis of the recovered catalyst was used to examine L-proline leaching in terms of nitrogen element percentage. About 3.92 wt% of  
30 elemental nitrogen was observed in the recovered catalyst, and this value was close to that in fresh catalyst (ca. 3.96 wt%). The inactivity of supernatants and the maintenance of the nitrogen element percentage in **catalyst 1** indicated that any leaching of active species into solution was insignificant. Further evidence of  
35 the stability of the magnetic L-proline catalyst was provided by the FT-IR spectra of fresh **catalyst 1** and **catalyst 1** reused five times (Fig. 7a vs. 7b). No significant change in catalyst occurred even after five times of reuse. TEM images (Fig. 2b' vs. 2b), as well as particle size analysis (Fig. 3b' vs. 3b), also showed that  
40 **catalyst 1** still maintained its nanostructure after repeated reuse. These observations suggested that the efficient **catalyst 1** was perfectly stable during the direct asymmetric aldol reaction and was readily recyclable from the reaction system.

45 **Table 3** Reuse of **catalyst 1** in the direct asymmetric aldol reaction of cyclohexanone with 2-nitrobenzaldehyde in water<sup>a</sup>

Entry	Run times	Yield <sup>b</sup> (%)	Anti/syn <sup>c</sup>	ee <sup>d</sup> (%)
1	Fresh	92	88:12	85
2	Second	95	89:11	84
3	Third	90	88:12	85
4	Fourth	90	88:12	85
5	Fifth	89	88:12	85

<sup>a</sup> **Catalyst 1** (10 mol% of 2-nitrobenzaldehyde), 2-nitrobenzaldehyde (0.25 mmol), cyclohexanone (2.5 mmol), H<sub>2</sub>O (2 ml), 12 h, 30 °C. <sup>b</sup> The same as Table 1. <sup>c</sup> The same as Table 1. <sup>d</sup> The same as Table 1.



50 **Fig. 7** FT-IR spectra of fresh **catalyst 1** (a) and **catalyst 1** reused five times (b).

## Conclusions

55 An efficient and magnetically recoverable L-proline catalyst was successfully prepared by immobilizing L-proline onto IL-modified MNPs. The presence of an IL linker in the supported L-proline catalyst resulted in excellent catalytic activity of the catalyst for a wide range of ketones and aromatic aldehydes in direct asymmetric aldol reaction in water without need for any  
60 organic solvent or additional additives. The catalyst can also be well dispersed in the reaction medium, easily magnetically recovered from the reaction mixture, and reused several times without significant loss of activity. All these advantages made the novel L-proline catalyst a green and promising organocatalyst for  
65 other important aqueous reactions.

## Experimental Section

### Materials and Reagents

4-Nitrobenzaldehyde, 2-chlorobenzaldehyde and 4-acetamidobenzaldehyde were obtained by TCI. 3-Bromopropylamine hydrobromide, 3-methoxybenzaldehyde, 2-nitrobenzaldehyde, 2-naphthaldehyde and 4-bromobenzaldehyde were bought from Acros. 3-Pentanone, cyclohexanone and cyclopentanone were purchased from Aldrich. N-[3-(triethoxysilyl)propyl]-4,5-dihydroimidazole, 3-aminopropyltriethoxysilane and tetraethyl orthosilicate (TEOS) were  
75 purchased from Alfa Aesa. Other commercially available chemicals were laboratory grade reagents from local suppliers. They were used without further purification, except for aromatic aldehyde, which was purified by distillation.

### Methods

80 <sup>1</sup>H NMR spectra of samples were recorded at a Varian-500 spectrometer. Fourier transform infrared (FT-IR) spectra were obtained as potassium bromide pellets with a resolution of 4 cm<sup>-1</sup> and 32 scans in the range 400–4000 cm<sup>-1</sup> using an AVATAR 370 Thermo Nicolet spectrophotometer. The thermogravimetric and differential thermogravimetric (TG-DTG) curves were obtained on a NETZSCH STA 449C thermal analyzer. Samples were heated from room temperature up to 700 °C under airflow using alumina sample holders. The sample weight was ca. 10 mg and the heating rate was 10 K/min. X-ray diffraction (XRD) patterns were

recorded on a Philips X' PERT-Pro-MPD diffractometer using Cu  $K_{\alpha}$  radiation ( $\lambda = 1.542 \text{ \AA}$ ). A continuous scan mode was used to collect 2 $\theta$  from 5 to 80°. The particle size and morphology of the samples were determined by transmission electronic microscopy (TEM, JEOL, JEM-200CX) with an acceleration voltage of 200 kV. The TEM samples for analysis were prepared by dropping the dilute suspensions of powders onto the carbon-coated copper grids and let the solvent evaporate. The average hydrodynamic diameter and size distribution of the samples were determined by a MS2000 Laser Particle Size Analyzer (Malvern, UK). The samples for measurement were sonicated in deionized water for 1.5 h. Analytical high performance liquid chromatography (HPLC) was carried out on Shimadzu LC-10A<sub>vp</sub> instrument using Daicel chiralpak OB-H, AD-H or AD columns.

### Preparation of Catalysts

**Preparation of (S)-N-(3-bromopropyl)-1-(tert-Butoxycarbonyl)pyrrolidine-2-carboxamide:** 3-Bromopropylamine hydrobromide (3.28 g, 15 mmol) was treated with 50 ml NaOH aqueous solution (10 wt.%) at 0 °C for 30 min. The liberated 3-bromopropylamine was extracted with dichloromethane (4 × 5 mL). N-Boc-L-proline (3.23 g, 15 mmol) was dissolved in dry THF (20 mL) and treated with triethylamine (1.5 g, 15 mmol). After cooling to 0 °C, ethyl chloroformate (1.62 g, 15 mmol) was slowly added over a period of 15 min. The mixture was stirred for another 30 min and then the solution of 3-bromopropylamine in dichloromethane was dropwise added. The resulting mixture was refluxed for 24 h. After removal of the formed white solid by filtration, the filtrate was concentrated in vacuo. The residue was dissolved in ethyl acetate (20 mL) and washed with water (3 × 20 mL), NaHCO<sub>3</sub> (3 × 20 mL) and NaCl (3 × 20 mL) in sequence. The combined organic layer was dried over anhydrous Na<sub>2</sub>SO<sub>4</sub>. After the evaporation of ethyl acetate, the residue was further purified by column chromatography (*n*-hexane: ethyl acetate = 2:1 (V/V)) to afford the (S)-N-(3-bromopropyl)-1-(tert-Butoxycarbonyl)pyrrolidine-2-carboxamide as a light yellow oil (3.9 g, 90% yield). Elemental analysis: Calc. for C<sub>13</sub>H<sub>23</sub>BrN<sub>2</sub>O: C, 46.58; H, 6.92; N, 8.36%. Found: C, 46.79; H, 6.75; N, 8.57%. <sup>1</sup>H NMR (D<sub>2</sub>O, 500MHz)  $\delta$  (ppm): 7.98 (t,  $J = 8.8$  Hz, 1H), 4.23 (t,  $J = 8.8$  Hz, 2H), 3.59 (t,  $J = 8.4$  Hz, 2H), 3.40 (t,  $J = 7.2$  Hz, 1H), 2.79 (t,  $J = 7.2$  Hz, 1H), 2.36 (m, 2H), 2.18 (m, 2H), 1.83 (t,  $J = 10.5$  Hz, 2H), 1.68 (t,  $J = 7.2$  Hz, 2H), 1.40 (s, 9H). FT-IR (KBr):  $\gamma_{\text{max}}/\text{cm}^{-1}$  3324, 2796, 1824, 1760, 1698, 1538, 1478, 1394, 1246, 1164, 1022, 977, 922, 881, 773, 644, 591, 547.

**Preparation of N-[3-(triethoxysilyl)propyl]-4,5-dihydroimidazole modified SiO<sub>2</sub>@Fe<sub>3</sub>O<sub>4</sub>:** SiO<sub>2</sub>@Fe<sub>3</sub>O<sub>4</sub> nanoparticles (2.5 g) was dispersed in 10 ml of dry toluene and sonicated for 30 min at room temperature. N-[3-(triethoxysilyl)propyl]-4,5-dihydroimidazole (2.74 g, 10 mmol) was then added. The mixture was refluxed for 24 h under nitrogen protection. After removal of dry toluene, the residue was washed with a large quantity of deionized water and ethanol (3 × 20 mL) by magnetic decantation, and dried under vacuum at room temperature overnight to yield the N-[3-(triethoxysilyl)propyl]-4,5-dihydroimidazole modified SiO<sub>2</sub>@Fe<sub>3</sub>O<sub>4</sub>. FT-IR (KBr):  $\gamma_{\text{max}}/\text{cm}^{-1}$  3749, 3440, 2929, 2864, 1655, 1560, 1540, 1456, 1434, 1399, 1131, 1040, 632, 581, 443.

**Preparation of catalyst 1:** The obtained N-alkylimidazole modified MNP was dispersed in dry toluene (30 ml). The solution of (S)-N-(3-bromopropyl)-1-(tert-Butoxycarbonyl)pyrrolidine-2-carboxamide (3.34 g, 10 mmol) in dry toluene (10 ml) was dropwise added into the above solution under vigorously stirring. The obtained mixture was refluxed for 12 h under nitrogen protection. After magnetic separation, the brown crude product was extracted thoroughly in toluene using a Soxhlet apparatus to remove homogeneous and unreacted start materials. The

solid was dried at 60 °C under vacuum for 24 h to give N-Boc-L-proline-IL-SiO<sub>2</sub>@Fe<sub>3</sub>O<sub>4</sub>. The obtained N-Boc-L-proline-IL-SiO<sub>2</sub>@Fe<sub>3</sub>O<sub>4</sub> was dispersed in dichloromethane (10 mL). Trifluoroacetic acid (TFA) (4.0 mL) was then added and the mixture was stirred at room temperature for 8 h. After removal of the solvent, the precipitate was washed completely with saturated NaHCO<sub>3</sub>, water and methanol for several times and dried in vacuum to get the **catalyst 1**. Elemental analysis: Found: C, 11.3; H, 1.61; N, 3.96%. FT-IR (KBr):  $\gamma_{\text{max}}/\text{cm}^{-1}$  2941, 2870, 1680, 1655, 1540, 1455, 1397, 1252, 1207, 1131, 1029, 834, 801, 638, 581.

**Preparation of the catalyst 2:** The IL-free counterpart of **catalyst 2**, in which L-proline was directly coupled to the amino-functionalized magnetic microspheres, was also prepared according to the similar preparation procedure of the **catalyst 1**. During the procedure, the organosiloxane of 3-aminopropyltriethoxysilane was used instead of the N-[3-(triethoxysilyl)propyl]-4,5-dihydroimidazole to modified the surface of the SiO<sub>2</sub>@Fe<sub>3</sub>O<sub>4</sub>. The abundant surface amino groups (-NH<sub>2</sub>) present on the SiO<sub>2</sub>@Fe<sub>3</sub>O<sub>4</sub> were readily reacted with the carboxyl group of the N-Boc-L-proline by the mixed anhydride method, giving the Boc-protected-L-prolinamide-SiO<sub>2</sub>@Fe<sub>3</sub>O<sub>4</sub>. Removal of the Boc-protecting group afforded the L-proline-NH<sub>2</sub>-SiO<sub>2</sub>@Fe<sub>3</sub>O<sub>4</sub> (denoted as **catalyst 2**). FT-IR (KBr):  $\gamma_{\text{max}}/\text{cm}^{-1}$  3390, 2926, 2877, 1680, 1557, 1540, 1517, 1455, 1427, 1397, 1207, 1131, 1037, 843, 634, 581, 443.

### General Procedure for the Direct Asymmetric Aldol Reaction

The selected catalyst (10 mol%, based on L-proline content in the catalyst), ketone (2.5 mmol), aldehyde (0.25 mmol) and deionized water (2 mL) were added in a 10 mL round-bottom flask in turn. The mixture was allowed to react at room temperature for 12 h. The reaction was monitored constantly by TLC. After completion of the reaction, the magnetic catalyst was separated by a magnet near the bottle. The reaction solution was removed from the reaction vessel by decantation while the external magnet held the magnetic catalyst inside the bottle. The magnetic catalyst was then washed with ethyl acetate, separated by magnetic decantation as described above, dried under vacuum overnight at room temperature for the recycle experiment. Ethyl acetate (3 × 10 mL) was used to extract the aldols from the reaction solution. The combined organic layers were washed with brine and dried with Na<sub>2</sub>SO<sub>4</sub>. After the evaporation of ethyl acetate, the residue was purified by column chromatography on silica gel (Acros, 40–60  $\mu\text{m}$ , 60  $\text{\AA}$ , eluent *n*-hexane/ethyl acetate = 3/1 (V/V)) to afford the desired aldol products. All products had the NMR spectra in agreement with published data. Enantiomeric excess of the corresponding aldol products was determined by HPLC analysis with a UV-vis detector using the Daicel chiralpak AD-H, OB-H or AD column. The syn and anti diastereomers of the aldols were readily distinguished in <sup>1</sup>H NMR spectroscopy by the diagnostic chemical shifts of -CHOH- proton. Detailed NMR spectra and HPLC analysis for aldol products are available in the Supporting Information.

**(2R,10S)-2-(Hydroxy-(2-nitrophenyl)methyl)cyclohexan-1-one 1.** Yield: 92%; (anti/syn) = 88: 12; ee value (anti): 85% determined by HPLC (Daicel chiralpak AD column; 2-propanol/*n*-hexane = 15: 85 (V/V)); flow rate = 1.0 mL/min; 25 °C;  $\lambda = 254$  nm;  $t_{\text{R}} = 13.4$  min (anti, major) and  $t_{\text{R}} = 14.2$  min (anti, minor). <sup>1</sup>H NMR (CDCl<sub>3</sub>, 500 MHz):  $\delta$  (ppm) 7.84 (d,  $J = 8.1$  Hz, 1H), 7.77 (d,  $J = 7.8$  Hz, 1H), 7.63 (t,  $J = 7.0$  Hz, 1H), 7.43 (t,  $J = 7.3$  Hz, 1H), 5.43 (d,  $J = 7.1$  Hz, 1H), 4.20 (s, 1H), 2.78-2.75 (m, 1H), 2.51-2.43 (m, 1H), 2.38-2.30 (m, 1H), 2.12-2.04 (m, 1H), 1.86-1.83 (m, 1H), 1.83-1.60 (m, 4H).

**(2R,10S)-2-(Hydroxy-(4-nitrophenyl)methyl)cyclohexan-1-one 2.** Yield: 96%; (anti/syn) = 76: 24; ee value (anti): 75% determined by HPLC (Daicel chiralpak AD column; 2-propanol/*n*-hexane = 15: 85 (V/V)); flow

rate = 1.0 mL/min; 25 °C;  $\lambda$  = 254 nm;  $t_R$  = 16.2 min (anti, major) and  $t_R$  = 21.4 min (anti, minor). <sup>1</sup>H NMR (CDCl<sub>3</sub>, 500 MHz):  $\delta$  (ppm) 8.21 (d,  $J$ =8.8 Hz, 2H), 7.51 (d,  $J$  = 8.8 Hz, 2H), 4.90 (dd,  $J$  = 8.4, 2.6 Hz, 1H), 4.08 (d,  $J$  = 3.1 Hz, 1H), 2.66-2.29 (m, 3H), 2.17-2.04 (m, 1H), 1.85-1.80 (m, 1H), 1.75-1.15 (m, 4H).

(2*R*,10*S*)-2-(Hydroxy-(2-chlorophenyl)methyl)cyclohexan-1-one **3**. Yield: 75%; (anti/syn) = 99:1; ee value (anti): 89% determined by HPLC (Daicel chiralpak AD column; 2-propanol/*n*-hexane = 10:90 (V/V)); flow rate = 1.0 mL/min; 25 °C;  $\lambda$  = 220 nm;  $t_R$  = 9.9 min (anti, major) and  $t_R$  = 11.1 min (anti, minor). <sup>1</sup>H NMR(CDCl<sub>3</sub>, 500 MHz):  $\delta$  (ppm) 7.84 (dd,  $J$ =7.8, 1.5 Hz, 1H), 7.34-7.28 (m, 2H), 7.21 (m, 1H), 5.36 (d,  $J$ =7.9 Hz, 1H), 4.03 (d,  $J$ =3.7 Hz, 1H), 2.72-2.67 (m, 1H), 2.48-2.44 (m, 1H), 2.38-2.31 (m, 1H), 2.11-2.04 (m, 1H), 1.84-1.81 (m, 1H), 1.70-1.54 (m, 4H).

(2*R*,10*S*)-2-(Hydroxy-(4-bromophenyl)methyl)cyclohexan-1-one **4**. Yield: 55%; (anti/syn) = 89:11; ee value (anti): 82% determined by HPLC (Daicel chiralpak AD column; 2-propanol/*n*-hexane = 10:90 (V/V)); flow rate = 1.0 mL/min; 25 °C;  $\lambda$  = 220 nm;  $t_R$  = 13.2 min (anti, minor) and  $t_R$  = 16.1 min (anti, major). <sup>1</sup>H NMR(CDCl<sub>3</sub>, 500 MHz):  $\delta$  (ppm) 7.48-7.45 (m, 2H), 7.21-7.18 (m, 2H), 4.75 (d,  $J$  = 8.6 Hz, 1H), 3.99 (d,  $J$  = 2.7 Hz, 1H), 2.60-2.52 (m, 1H), 2.51-2.43 (m, 1H), 2.40-2.30 (m, 1H), 2.13-2.06 (m, 1H), 1.85-1.74 (m, 1H), 1.73-1.49 (m, 3H), 1.34-1.25 (m, 1H).

(2*R*,10*S*)-2-(Hydroxy-(2-naphthyl)methyl)cyclohexan-1-one **5**. Yield: 30%; (anti/syn) = 98:2; ee value (anti): 45% determined by HPLC (Daicel chiralpak AD column; 2-propanol/*n*-hexane = 2:98 (V/V)); flow rate = 1.0 mL/min; 25 °C;  $\lambda$  = 220 nm;  $t_R$  = 26.2 min (anti, major) and  $t_R$  = 29.6 min (anti, minor). <sup>1</sup>H NMR(CDCl<sub>3</sub>, 500 MHz):  $\delta$  (ppm) 7.75-7.85 (m, 4H), 7.46-7.50 (m, 3H), 5.01(d,  $J$  = 8.7 Hz, 1H), 4.10 (s, 1H), 2.71-2.78 (m, 1H), 2.37-2.55 (m, 2H), 2.09-2.14 (m, 1H), 1.52-1.80 (m, 5H), 1.28-1.42 (m, 2H).

(2*R*,10*S*)-2-(Hydroxy-(4-nitrophenyl)methyl)cyclopentan-1-one **6**. Yield: 90%; (anti/syn) = 33:67; ee value (anti): 86% determined by HPLC (Daicel chiralpak AD column; 2-propanol/*n*-hexane = 10:90 (V/V)); flow rate = 1.0 mL/min; 25 °C;  $\lambda$  = 220 nm;  $t_R$  = 12.9 min (anti, major) and  $t_R$  = 16.7 min (anti, minor). <sup>1</sup>H NMR(CDCl<sub>3</sub>, 500 MHz):  $\delta$  (ppm) 8.21-8.19 (m, 2H), 7.54-7.51 (m, 2H), 5.42 (d,  $J$ =9.0 Hz, 1H), 4.86 (s, 1H), 2.49-1.99(m, 3H), 2.08-1.95 (m, 1H), 1.76-1.25 (m, 3H).

(4*R*)-Hydroxy-4-(2-nitrophenyl)-butan-2-one **7**. Yield: 93%; ee value: 79% determined by HPLC (Daicel chiralpak OB-H column; 2-propanol/*n*-hexane = 15:85 (V/V)); flow rate = 1 mL/min; 25 °C;  $\lambda$  = 254 nm;  $t_R$  = 7.3 min (minor) and  $t_R$  = 8.4 min (major). <sup>1</sup>H NMR (CDCl<sub>3</sub>, 500 MHz):  $\delta$  (ppm) 7.95-7.42 (m, 4H), 5.68 (d,  $J$ =10.7Hz, 1H), 3.73 (s, 1H), 3.15-2.72 (m, 2H), 2.24 (s, 3H).

(4*R*)-Hydroxy-4-(4-nitrophenyl)-butan-2-one **8**. Yield: 96%; ee value: 70% determined by HPLC (Daicel chiralpak OB-H column; 2-propanol/*n*-hexane = 15:85 (V/V)); flow rate = 1 mL/min; 25 °C;  $\lambda$  = 254 nm;  $t_R$  = 14.7 min (major) and  $t_R$  = 16.9 min (minor). <sup>1</sup>H NMR (CDCl<sub>3</sub>, 500 MHz):  $\delta$  (ppm) 8.22-7.28 (m, 4H), 5.27 (s, 1H), 3.67 (s, 1H), 2.87 (d,  $J$ =6.7Hz, 2H), 2.23 (s, 3H).

(4*R*)-(2-Chlorophenyl)-4-hydroxy-2-butanone **9**. Yield: 75%; ee value: 77% determined by HPLC (Daicel chiralpak AD column; 2-propanol/*n*-hexane = 7.5:92.5 (V/V)); flow rate = 0.8 mL/min; 25 °C;  $\lambda$  = 254 nm;  $t_R$  = 10.9 min (major) and  $t_R$  = 12.3 min (minor). <sup>1</sup>H NMR (CDCl<sub>3</sub>, 500 MHz):  $\delta$  (ppm) 7.61-7.19 (m, 4H), 5.52-5.49 (m, 1H), 3.63 (s, 1H), 3.00-2.65 (m, 2H), 2.21(s, 3H).

(4*R*)-(4-Bromophenyl)-4-hydroxy-2-butanone **10**. Yield: 55%; ee value: 77% determined by HPLC (Daicel chiralpak AD column; 2-propanol/*n*-hexane = 7.5:92.5 (V/V)); flow rate = 0.8 mL/min; 25 °C;  $\lambda$  = 254 nm;  $t_R$

= 15.2 min (major) and  $t_R$  = 16.1 min (minor). <sup>1</sup>H NMR (CDCl<sub>3</sub>, 500 MHz):  $\delta$  (ppm) 7.47-7.21 (m, 4H), 5.10 (d,  $J$  = 8.7Hz, 1H), 3.43 (s, 1H), 2.86-2.76 (m, 2H), 2.19 (s, 3H).

(4*R*)-(4-Acetamidophenyl)-4-hydroxy-2-butanone **11**. Yield: 35%; ee value: 83% determined by HPLC (Daicel chiralpak AD column; 2-propanol/*n*-hexane = 10:90 (V/V)); flow rate = 0.8 mL/min; 25 °C;  $\lambda$  = 254 nm;  $t_R$  = 50.0 min (major) and  $t_R$  = 55.7 min (minor). <sup>1</sup>H NMR (CDCl<sub>3</sub>, 500 MHz):  $\delta$  (ppm) 7.47-7.26 (m, 4H), 5.12-5.11 (m, 1H), 3.34 (s, 1H), 2.89-2.77 (m, 2H), 2.20 (s, 3H), 2.17 (s, 3H).

(4*R*)-Hydroxy-4-(2-naphthyl)-2-butanone **12**. Yield: 32%; ee value: 82% determined by HPLC (Daicel chiralpak AD column; 2-propanol/*n*-hexane = 7.5:92.5 (V/V)); flow rate = 0.8 mL/min; 25 °C;  $\lambda$  = 254 nm;  $t_R$  = 22.6 min (major) and  $t_R$  = 27.0 min (minor). <sup>1</sup>H NMR (CDCl<sub>3</sub>, 500 MHz):  $\delta$  (ppm) 7.80-7.43 (m, 7H), 5.31-5.29 (m, 1H), 3.50 (s, 1H), 2.96-2.84 (m, 2H), 2.18 (s, 3H).

## Acknowledgements

The project was financially supported by the National Natural Science Foundation of China (Grant No. 21003044, 20973057), the Natural Science Foundation of Hunan Province (10JJ6028) and the Program for Science and Technology Innovative Research Team in Higher Educational Institutions of Hunan Province. The authors are grateful to Dr. Qiang Gao (China University of Geosciences) for his help with the characterization with TEM.

## Notes and references

- [1] (a) R. Mahrwald, *Chem. Rev.*, 1999, **99**, 1095; (b) T. D. Machajewski and C. H. Wong, *Angew. Chem. Int. Ed.*, 2000, **39**, 1352; (c) Z. Tang, Z. Yang, X. Chen, L. Cun, A. Mi, Y. Jiang and L. Gong, *J. Am. Chem. Soc.*, 2005, **127**, 9285; (d) E. G. Doyagüez and A. F. Mayoralas, *Tetrahedron*, 2012, **68**, 7345.
- [2] (a) B. List, R. A. Lerner and C. F. Barbas III, *J. Am. Chem. Soc.*, 2000, **122**, 2395; (b) K. Sakthivel, W. Notz, T. Bui and C. F. Barbas III, *J. Am. Chem. Soc.*, 2001, **123**, 5260; (c) Z. Tang, F. Jiang, L. Yu, X. Cui, L. Gong, A. Mi, Y. Jiang and Y. Wu, *J. Am. Chem. Soc.*, 2003, **125**, 5262; (d) B. Alcaide and P. Almendros, *Angew. Chem. Int. Ed.*, 2003, **42**, 858; (e) N. Mase, Y. Nakai, N. Ohara, H. Yoda, K. Takabe, F. Tanaka and C.F. Barbas III, *J. Am. Chem. Soc.*, 2006, **128**, 734; (f) S. S. Khan, J. Shah and J. Liebscher, *Tetrahedron*, 2010, **66**, 5082; (g) S. Calogero, D. Lanari, M. Orrù, O. Piermatti, F. Pizzo and L. Vaccaro, *J. Catal.*, 2011, **282**, 112; (h) G. Chen, X. Fu, C. Li, C. Wu and Q. Miao, *J. Organomet. Chem.*, 2012, **702**, 19; (i) S. Z. Luo, X. L. Mi, L. Zhang, S. Liu, H. Xu, and J. Cheng, *Angew. Chem. Int. Ed.* 2006, **45**, 3093.
- [3] (a) A. Berkessel, B. Koch and J. Lex, *Adv. Synth. Catal.*, 2004, **346**, 1141; (b) Z. Tang, F. Jiang, X. Cui, L. Gong, A. Mi, Y. Jiang and Y. Wu, *Proc. Natl. Acad. Sci. U.S.A.*, 2004, **101**, 5755; (c) D. Gryko and R. Lipiński, *Eur. J. Org. Chem.*, 2006, **17**, 3864.
- [4] (a) G. Yang, Z. Yang, L. Zhou, R. Zhu and C. Liu, *J. Mol. Catal. A: Chem.*, 2010, **316**, 112; (b) H. Yang, S. Li, X. Wang, F. Zhang, X. Zhong, Z. Dong and J. Ma, *J. Mol. Catal. A: Chem.*, 2012, **363**, 404.
- [5] (a) P. Kotrusz, I. Kmentová, B. Gotov, Š. Toma and E. Solčániová, *Chem. Commun.*, 2002, **21**, 2510; (b) T. Loh, L. Feng, H. Yang and J. Yang, *Tetrahedron Lett.*, 2002, **43**, 8741; (c) M. Lombardo, F. Pasi, S. Easwar and C. Trombini, *Adv. Synth. Catal.*, 2007, **349**, 2061; (d) J. Shah, H. Blumenthal, Z. Yacob and J. Liebscher, *Adv. Synth. Catal.*, 2008, **350**, 1267.
- [6] (a) S. Aratake, T. Itoh, T. Okano, N. Nagae, T. Sumiya, M. Shoji and Y. Hayashi, *Chem. Eur. J.*, 2007, **13**, 10246; (b) M. Amedjkouh, *Tetrahedron: Asymmetry*, 2007, **18**, 390; (c) D. E. Siyutkin, A. S. Kucherenko and S. G. Zlotin, *Tetrahedron*, 2009, **65**, 1366.
- [7] (a) D. E. Siyutkin, A. S. Kucherenko, M. I. Struchkova and S. G. Zlotin, *Tetrahedron Lett.*, 2008, **49**, 1212; (b) D. E. Siyutkin, A.S. Kucherenko and S.G. Zlotin, *Tetrahedron.*, 2010, **66**, 513.

- [8] (a) U. Laska, C. G. Frost, G. J. Price and P. K. Plucinski, *J. Catal.*, 2009, **268**, 318; (b) D. Li, W. Y. Teoh, J. J. Gooding, C. Selomulya and R. Amal, *Adv. Funct. Mater.*, 2010, **20**, 1767; (c) Y. Zhu, L. P. Stubbs, F. Ho, R. Liu, C. P. Ship, J. A. Maguire and N. S. Hosmane, *ChemCatChem*, 2010, **2**, 365; (d) S. Shylesh, V. Schünemann and W. R. Thiel, *Angew. Chem. Int. Ed.*, 2010, **49**, 3428; (e) Y. Zhu, L. Tian, Z. Jiang, Y. Pei, S. Xie, M. Qiao and K. Fan, *J. Catal.*, 2011, **281**, 106; (f) M. Z. Kassaei, H. Masrouei and F. Movahedi, *Appl. Catal. A*, 2011, **395**, 28; (g) V. Polshettiwar, R. Luque, A. Fihri, H. Zhu, M. Bouhrara and J. Basset, *Chem. Rev.*, 2011, **111**, 3036; (f) M. B. Gawande, V. D. B. Bonifácio, R. S. Varma, I. D. Nogueira, N. Bundaleski, C. A. A. Ghumman, O. M. N. D. Teodoro and P. S. Branco, *Green Chem.*, 2013, DOI:10.1039/C3GC40375K; (g) S. Z. Luo, X. X. Zeng and J. Cheng, *Chem. Commun.*, 2008, 5719.
- [9] (a) S. Luo, X. Zheng, H. Xu, X. Mi, L. Zhang and J. Cheng, *Adv. Synth. Catal.*, 2007, **349**, 2431; (b) S. Luo, X. Zheng and J. Cheng, *Chem. Commun.*, 2008, **44**, 5719; (c) O. Gleeson, R. Tekoriute, Y. K. Guňko, and S. J. Connon, *Chem. Eur. J.*, 2009, **15**, 5669; (d) V. Polshettiwar, B. Baruwati and R. S. Varma, *Chem. Commun.*, 2009, **14**, 1837; (e) S. Shylesh, V. Schünemann and W. R. Thiel, *Angew. Chem. Int. Ed.*, 2010, **49**, 3428; (f) B. G. Wang, B. C. Ma, Q. Wang and W. Wang, *Adv. Synth. Catal.*, 2010, **352**, 2923.
- [10] (a) Y. Gu and G. Li, *Adv. Synth. Catal.*, 2009, **351**, 817; (b) P. Virtanen, H. Karhu, G. Toth, K. Kordas and J. P. Mikkola, *J. Catal.*, 2009, **263**, 209; (c) M. I. Burguete, E. García-Verdugo, I. García-Villar, F. Gelat, P. Licence, S.V. Luis and V. Sans, *J. Catal.*, 2010, **269**, 150.
- [11] (a) S. Bahmanyar, K. N. Houk, H. J. Martin and B. List, *J. Am. Chem. Soc.*, 2003, **125**, 2475; (b) S. Aratake, T. Itoh, T. Okano, T. Usui, M. Shoji and Y. Hayashi, *Chem. Commun.*, 2007, **24**, 2524.
- [12] X. Liu, Z. Ma, J. Xing and H. Liu, *J. Magn. Magn. Mater.*, 2004, **270**, 1.
- [13] Y. H. Deng, D. W. Qi, C. H. Deng, X. M. Zhang and D. Y. Zhao, *J. Am. Chem. Soc.*, 2008, **130**, 28.
- [14] D. Gryko and R. Lipiński, *Adv. Synth. Catal.*, 2005, **347**, 1948.
- [15] D. Yuan, Q. Zhang and J. Dou, *Catal. Commun.*, 2010, **11**, 606.
- [16] Q. Zeng, I. Baker and J. Hoopes, *Mater. Res. Soc. Symp. Proc.*, 2007, **962**, 10.
- [17] N. T. S. Phan and C. W. Jones, *J. Mol. Catal. A: Chem.*, 2006, **253**, 123.
- [18] Y. Zhang, Y. Zhao and C. Xia, *J. Mol. Catal. A: Chem.*, 2009, **306**, 107.
- [19] K. Su, T. Pan and Y. Zhang, *The Analytic Method of Spectrum, 1st ed.*, (Eds.: G. Rong) East China Univ. of Science & Technology Press, 2002, p. 106.
- [20] R. Luo, R. Tan, Z. Peng, W. Zheng, Y. Kong and D. Yin, *J. Catal.*, 2012, **287**, 170.
- [21] G. Wang, N. Yu, L. Peng, R. Tan, H. Zhao, D. Yin, H. Qiu, Z. Fu and D. Yin, *Catal. Lett.*, 2008, **123**, 252.
- [22] (a) Y. Gu, C. Ogawa, J. Kobayashi, Y. Mori, Shu Kobayashi, *Angew. Chem. Int. Ed.*, 2006, **45**, 7217; (b) Y. Chi, S. T. Scroggins, E. Boz and J. M. J. Fréchet, *J. Am. Chem. Soc.*, 2008, **130**, 17287; (c) J. Tan, H. Li and Y. Gu, *Green Chem.*, 2010, **12**, 1772.
- [23] (a) N. Zotova, A. Franzke, A. Armstrong and D. G. Blackmond, *J. Am. Chem. Soc.*, 2007, **129**, 15100; (b) G. Angelici, R. J. Corrêa, S. J. Garden and C. Tomasini, *Tetrahedron Lett.*, 2009, **50**, 814.
- [24] A. R. Siamaki, A. E. R. S. Khder, V. Abdelsayed, M. S. El-Shall and B. F. Gupton, *J. Catal.*, 2011, **279**, 1.
- [25] G. Liu, H. Zhao, Y. Lan, B. Wu, X. Huang, J. Chen, J. Tao and X. Wang, *Tetrahedron*, 2012, **68**, 3843.